16th World Conference on Earthquake, 16WCEE 2017

Santiago Chile, January 9th to 13th 2017

Paper N° 343

Registration Code: 170794599

GRANULAR MECHANICS OF THE SEISMIC LATERAL EARTH PRESSURE ON RIGID RETAINING WALLS

C. Yanqui[1]

[1] *Professor, San Agustin National University of Arequipa, cyanquimurillo@hotmail.com*

Abstract

Small scale experiments, ran by different authors on the seismic behavior of retaining walls, have led to the conclusion that the distribution of the active lateral soil pressure exhibits a nonlinear tendency, and is highly dependent on the kinematics of the wall; despite of the assumptions of the Mononobe-Okabe method. In this paper, both of these features are explained in a direct and simple way by means of the Granular Mechanics, whose principal hypothesis is the transmission of stresses as chains of forces of contact between grains, which has been experimentally confirmed by the photographs taken on packings of birefringent disks. Previously, by applying the principle of the mean value, it is demonstrated that any function in a disordered discontinuum can be attained as it were in a crystalline substance, whose cell parameters are defined by the variances and covariances of the original fabric metrics. Regarding this result, the random chains of contact forces, inherent to dense soils, are treated as they were linear, conjugate and ordered. When they are associated to their geometric domain of influence, chains come to be bands of contact forces, The pseudo-statics of these bands provides the stresses for a linearly bounded soil mass, in “at rest” condition, or Rankine´s plastic state. A shear band shows up if only one band of contact forces reaches the plastic state. This is the case of the backfill at limit equilibrium, where a plastic band separates the mobilized wedge from the unstrained soil. On this basis, by applying just the law of sines to the quantities involved, a general bilinear equation for the seismic earth lateral pressure is deduced, which may be specialized for the three elementary movements of the rigid wall: rotation about the base, horizontal translation, and rotation about the top. The kinematics of the grains in the rhomboid cell, relative to the movement mode, defines the inclination of the contact forces, and, hence, the inclination of the respective band. In the first mode of movement, the pressure distribution is linear, but the lateral force resultant is larger than the Monobe-Okabe´s. In the second and third modes, the earth pressure distribution is bilinear with the maximum value near the base and near the top, respectively. In the third mode, the bands inclined toward the back side of the retaining wall are deduced to be in passive plastic state. For rotating walls, two modes of inter-grains movements are possible, giving rise to a semi-plastic state and a full plastic state of the soil mass, that, regarding the energy involved, are related to moderate and severe earthquakes, respectively. Finally, the lateral earth pressure and the resultant force, obtained in this theory, are compared with the published experimental data, showing a good agreement.

Keywords: Discontinuum; granular mechanics; force bands; earth pressure; grains kinematics

1. Introduction

The determination of earth pressure in highly seismic regions of the Earth is a problem not yet solved satisfactorily. Since the pioneering work of Okabe [1], and the careful testing scaled made by Mononobe and Matsuo [2], which showed an increase of earth pressure against the wall under dynamic conditions, several theories have been proposed to explain this behavior. The Mononobe-Okabe method, which is an extension of the static method of Coulomb, is the oldest and has been used for several decades; but it has also been criticized by several authors due to the following limitations [3]: a) the theory is pseudo-static; b) it can predict the earth pressure only under moderate earthquakes, because, for strong earthquake ground motions, the theory yields low values, not consistent with reality; c) formation of the failure plane into the backfill soil is instantaneous with simultaneous mobilization of the friction angle along the failure plane; and d) the theory is based on the assumption that the failure surface is planar. Although this assumption leads to obtaining coefficient values of active lateral earth pressures close to those obtained from a theoretical curved surface, it can not be true for calculating the coefficient of lateral stress under seismic loads.

To overcome these shortcomings, some authors have proposed various hypotheses, in the frameworks of the plasticity and elasticity theories. For example, Koseki et al. [4] proposed a modified pseudo-static limit equilibrium method, to include the effect of the strain localization or shear band in the backfill, and the reduction of the peak friction angle. Zhang and Li [5] adopted a similar approach, and mathematically evaluated the effect of strain localization on the Mononobe-Okabe method. Fang and Chen [6] modified this method to take into consideration the effect of the inertial forces. Ichihara et al. [7] extended the rigorous Sokolovski´s theory, that obeys the Mohr-Coulomb law at each point, to the dynamic problem of plastic backfills. In this paper, a different approach is presented, which is based on the granular and discontinuous nature of soils. Both of the latter theories satisfy the equilibrium equations and the boundary conditions.

2. Behavior of dense granular soils

Dense soils exhibit two properties more, in addition to those already known [8]: a) multiplicity, by which, the grains assemblage changes depending on the kind of stress and the strain level of the soil mass, b) arching, by which, the stress transmission is accomplished as chains of contact forces. These properties can be evidenced, for example, in the photographs taken on the two-dimensional specimens of packings made of regularly or randomly distributed photo-elastic disks [9] (Figure 1a). They can also be obtained through simulation schemes called contact dynamics and molecular dynamics [10].

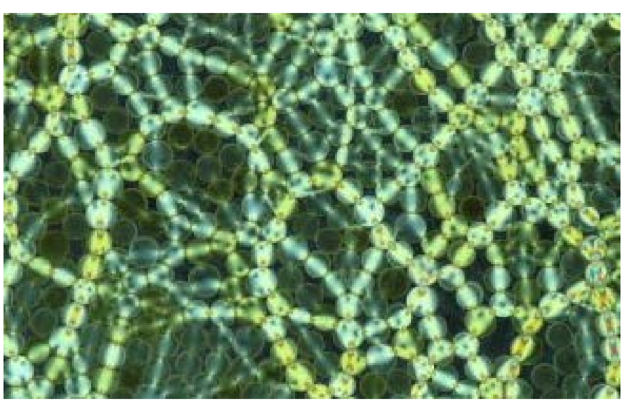

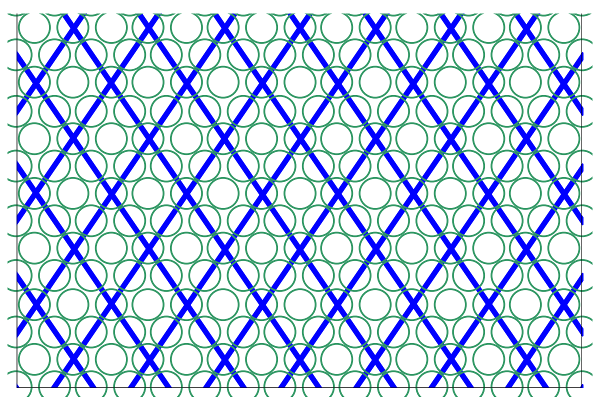

Fig. 1. a) Photograph of the chains of contact forces in a granular substance of random birefringent spheres [9]; b) Equivalent ordered granular medium, statistically transformed by the mean value principle

In general, this special behavior of granular soils can not be explained by means of the continuum mechanics, although several models have been proposed, such as the Terzaghi´s theory of "arching effect". Better models are those that take into account the granular nature of this substance; for instance, the physics of granular matter, which uses the concepts of statistical mechanics [11], or the numerical methods, that are the most common method for the study of grain-level properties of granular matter [12]. But both of these methods are not suitable for the practical engineer. So that, some authors have struggled to develop a simple and direct method, called granular mechanics. In this framework, pioneering works of Trollope [13] and Rowe [14] on the transmission of forces should be highlighted.

3. Discontinuum mechanics

All bodies existing in nature are composed of particles and interstices. The particles are units of matter concentration and the interstices are the spaces not occupied by the particles. According to the distribution of these units, called nodes, discontinuous media can be ordered or crystalline, and disordered or random. Soils are of the second type. One distinguishing feature of this media is the principle of the mean value, by which a function describing any phenomenon or state: $f = f(\boldsymbol{r})$, where $\boldsymbol{r}$ is the position vector of the node, can be assessed. As long as the laws governing a phenomenon are unknown, or they are so complicated that they are not of practical application, the position function, f, at the $\boldsymbol{r}$ node, can be estimated by averaging the f_i values corresponding to the N neighboring nodes, located near node $\boldsymbol{r}$, and belonging to the domain D, called the domain of homogeneity or sample space. The function $fi = f(\boldsymbol{r}+ \boldsymbol{a_i})$, where $\boldsymbol{a_i}$ is the distance from node $\boldsymbol{r}$ to node $\boldsymbol{r_i}$, can be expressed in terms of the derivatives of f using the Taylor´s expansion. The differential equation obtained in this way highlights the fact that if the magnitude of $\boldsymbol{a_i}$ is comparable to body size, the higher order terms are important; but if the number of homologous points is very large, the first term is enough, yielding, for two-dimensional problems, the differential equation of the mean value [15]:

$$m_{xx}\frac{\partial^2 f}{\partial x^2}+2m_{xz}\frac{\partial^2 f}{\partial x \partial z}+m_{zz}\frac{\partial^2 f}{\partial z^2}=0 \quad ; \qquad m_{jk}=\frac{2}{N}\sum_{i=1}^{N/2} a_{ji}a_{ki} \tag{1}$$

The coefficients, m_{jk}, of this equation are the components of the fabric metric tensor, belonging to the sample domain D, where a_{ji} and a_{ki} are the Cartesian components of the vector $\boldsymbol{a_i}$. Examination of these equations leads to the following conclusions: first, the principle of the mean value transforms a discontinuum into an anisotropic continuum; second, the coefficients of this equation correspond to the second statistical moments, namely, the variances and covariances of the Cartesian metric components of the nodes belonging to the sample domain D; third, except for the coefficients, the equation of the mean value is the same, regardless of the number of nodes contained in the sample domain D, which means that a medium of random structure behaves as it were crystalline medium. This conclusion reveals that, in granular substance, the random paths of the chains of contact forces can be modeled as linear paths of conjugated chains of contact forces; or, for the sake of the stress calculation, bands of contact forces, defined by the θ_1 and θ_2 directions (Fig. 1.b).

4. Contact forces in a granular medium

For a bi-dimensional pseudo-static problem, components of stress tensor may be calculated by solving the system of three differential equations: the equation of the mean value (1), in which the function f is any of the components of the stress tensor, and the two equations of equilibrium, deduced for a medium with two components of the body force per unit volume, $g_x = \gamma\alpha_h$ and $g_z = \gamma(1\text{-}\alpha_v)$, where γ is the unit weight of soil and α_h and α_v, the horizontal and vertical seismic coefficients, respectively

A more simple and direct way to get these stress components in dense granular soils is using the linear chains of contact forces, which can be calculated using the methods of elementary statics. The first step is to determine the weight of the rhomboidal cell in terms of the volume of the conjugate basic element of each band of contact forces: $W_0=\gamma S_1 h_2=\gamma S_2 h_1$, where S_1, h_1, S_2, and h_2 are the bases and the heights of the parallelogram in the directions 1, and, 2, respectively. The second step is the composition of the weight and the maximum inertia force to find the resultant $\boldsymbol{R_0} = W_0[\alpha_h \boldsymbol{i}+(1\text{-}\alpha_v)\boldsymbol{j}]$. The third step is the resolution of this force into the contact forces, f_1 and f_2, along the direction of the conjugated chains (Fig.2a). The fourth step is the calculation of the band forces F_1 and F_2 by adding all the contact forces contained in each direction, to find:

$$F_1 = \frac{\gamma(1-\alpha_v)S_1 z_1 \sin(\theta_2 + s)}{\cos s \sin(\theta_1 + \theta_2)} \quad ; \quad F_2 = \frac{\gamma(1-\alpha_v)S_2 z_2 \sin(\theta_1 + s)}{\cos s \sin(\theta_1 + \theta_2)} \tag{2}$$

where $z_1 = N_1 h_2$ and $z_2 = N_2 h_1$ are the heights of the conjugate bands converging at the node (x, z) (Fig. 2.b), and θ_1 and θ_2 are the directions of the chain forces . As a custom, for convenience, α_h is expressed in terms of α_v in these equations, through the parameter s, which is an angle defined as follows: tan $s = \alpha_h /(1-\alpha_v)$.

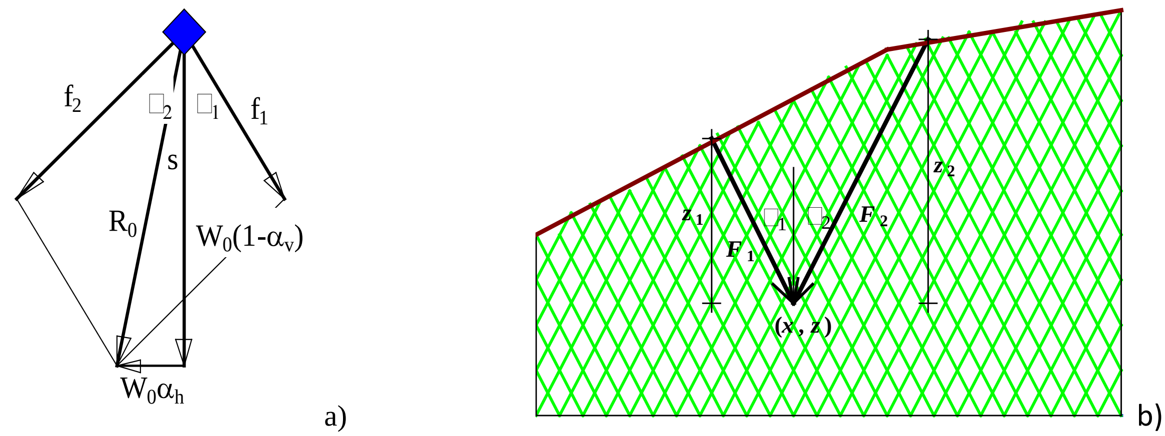

Fig. 2. a) Contact forces in a rhomboid element caused by its own weight and the maximum seismic inertia force. b) Bands of contact forces in a bilinear soil slope.

5. Pseudo-static stress state

The stress components are determined dividing each band force by the area of the band section, S_i; and then algebraically adding the results. This operation becomes more compact and elegant by using the Cartesian tensor nomenclature. On this purpose, the directions of the bands should be described by the unit vectors $\boldsymbol{u_k}$, whose Cartesian components are the direction cosines, u_{jk}, that are called the elements of the structural matrix. Then, the solution to the system of two equations obtained from the resolution of the body force into the direction of the bands yields the forces chains: F_1 and F_2. Dividing these forces between the areas of the sections parallel to the Cartesian axes, taking account of the relationship that they keep in terms of cosines directors, the three stress components, σ_{jk}, are obtained in a single expression, using indicial notation [16]:

$$\sigma_{jk} = \frac{1}{U}\sum_{m=1}^{2}\sum_{n=1}^{2}\frac{g_m U_{mn}}{u_{mn}} u_{jn} u_{kn} z_n \tag{3}$$

where g_m are the Cartesian components of the mass forces acting on the medium, assuming the values m=1 and m=2 for the vertical and horizontal directions, respectively; z_n, is the height of the inclined n column; U, the determinant of the structural matrix, u_{jk}; and U_{mm}, the cofactors of the mn element of this matrix. As can be verified by direct derivation, the stress components, calculated in this way, satisfy the differential equations of equilibrium.

6. Inclination of the bands of contact forces

In the above analysis, it is shown that all equations depend on the angles of inclination of the bands of contact forces, which are the fundamental parameters of a granular medium and are not yet known. The easiest way to find them consists in appealing to some known experimental or observational data; for example, the stresses within an infinite soil slope. For a soil mass, modeled as a medium consisting of conjugated symmetrical bands, defined by the parameter η = cot θ, where $\theta = \theta_1 = \theta_2$, and limited by a linear slope m = tan i, the stress components are obtained from eq. (3) as:

$$\sigma_x = \frac{\gamma z(1-\alpha_v + m\alpha_h)}{\eta^2 - m^2} \quad ; \qquad \sigma_z = \eta^2 \sigma_x \; ; \qquad \tau_{xz} = \frac{\gamma z[(1-\alpha_v)m + \alpha_h \eta^2]}{\eta^2 - m^2} \tag{4}$$

If the soil mass is in plastic state, the angle θ of the plastic bands of contact forces, $\theta = \theta_f$, can be calculated introducing the stress components in the Mohr-Coulomb law, and solving θ_f in terms of the angle of internal friction, φ, as follows:

$$\cos 2\theta_f = \sin(i+s)\sin(i-s) \pm \cos(i-s)\sqrt{\cos^2(i+s) - \cos^2\varphi} \tag{5}$$

The square root giving by this formula is real if the maximum inclination of the soil slope is: $i = \varphi - s$.

When the soil mass is "at rest" condition, the angle θ remains constant regardless of the inclination of the slope. In this condition, the soil mass is not at failure state, except at the critical inclination of the soil slope, which coincides with the maximum value of the plastic state, giving by eq. (5). So that, the angle for the at rest condition, $\theta = \theta_0$, is attained as:

$$\cos 2\theta_0 = \sin\varphi \sin(\varphi - 2s) \tag{6}$$

7. Shear bands

Experimentally, it has been found that dense granular soils submitted to some stress state exhibit zones of localized strain called shear bands. The formation and evolution of these bands are usually studied using fracture mechanics, bifurcation theory, or fractals dimensions [17, 18]. But these theories are not suited for direct and easy apprehension. In the granular mechanics, a localized deformation zone shows up as a natural consequence of the theory of matter made of bands, when only one or two bands come to be plasticized, while the rest of the soil remains in another mechanical state. As long as this band is not the consequence of a shear strain alone, but principally due to the rotation of grains with respect to the contact points, it is more appropriate to call it plastic band. This begins as a localized deformation at a singular point, such as the corner of the retaining wall heel, and then runs in the direction of the band involved. Consequently, for dense soils that obey the Mohr-Coulomb law along the plastic band, it is concluded that the inclination of this band is given by equation (5). Also, it is concluded that the significance of a plastic band is different from a slip line, although both may coincide in direction for some cases, such as the soil mass bounded by a horizontal surface.

8. Kinematics of the retaining walls

Careful tests conducted by several authors with granular backfills, have shown that the distribution of the lateral pressure on the back face of the retaining wall depends on the kinematics of the wall. Currently, it is entirely clear that the wall, as a rigid body, may undergo three types of movement: horizontal translation (T), rotation about the base (RB), and rotation about the top (RT). In all cases, a limit plastic band separates the mobilized wedge from the rest of the soil mass, which remains fixed and unstrained. Then, the cinematic boundary conditions require that both the back side of the retaining wall and the limit plastic band remain linear after the translation or the rotation. To satisfy these conditions, grains in a basic cell should appropriated translate or rotate with respect to the neighbors.

8.1 Rotation about the base (RB)

Two strain mechanisms are plausible. a) The upper grain is indented symmetrical and vertically into the pore displayed by the two lower grains of the assemblage. At the failure state, the conjugate force chains assume the angles: $\theta_1 = \theta_2 = \theta_f$. In this case, the entire free surface of the strained wedge is depressed, forming a graben consisting of a mass of conjugate plastic bands. b) The upper grain rotates in counterclockwise direction with respect to the point of contact with the lower right grain. This rotation is possible only if each upper grain slides respect to the lower left grain. Hence, an “at rest” contact force results in the direction to the fixed soil, and a plastic contact force, in the direction of the retaining wall. Respectively, $\theta_1 = \theta_0$ and $\theta_2 = \theta_f$. Such a soil mass is said to be in semi-plastic state. Externally, the ground surface rotates about the upper end of the limit plastic band, overtaking the maximum vertical displacement at the top of the wall back face. In both mechanisms, the distribution of the earth lateral pressure is lineal (Fig. 6a)

Clearly, the development of the first strain mechanism requires more energy than the second. Therefore, it is concluded that the first strain mechanism is associated to the severe earthquakes, while the second, to the moderate ones. Indeed, several authors have found that, from a certain seismic acceleration, the trend on the relationship between the seismic lateral force and the seismic coefficient changes. For example, Noda et al. [19], based on the case histories of 129 gravity type quay walls submitted to 12 different earthquakes, found that the threshold acceleration approaches 0.2g; while Matsuo and Itabashi [20], based on the inverse analysis, proposed that the parameter *s* be obtained as an empirical linear relationship. In this paper, it is assumed a threshold value of 0.25g, based on the experimental data detailed below, which show a change of the seismic coefficient between 0.2g and 0.3g, approximately (Figs. 6b and 7).

8.2 Horizontal translation (T)

Only one mechanism is plausible: grains remain at the “at rest” condition even at failure state. So that, the conjugate contact forces assume the angles $\theta_1 = \theta_2 = \theta_0$. The strained wedge slides down as a rigid body relative to the retaining wall and to the fixed soil, drawing a graben. Since $\theta_0 > \theta_f$, the mobilized wedge comes to be divided into two zones, with two different contours: the ground surface and the limit plastic band. Consequently, the distribution of the earth lateral pressure is bilinear, becoming zero at the top and at the bottom of the retaining wall (Fig. 4).

8.3 Rotation about the top (RT)

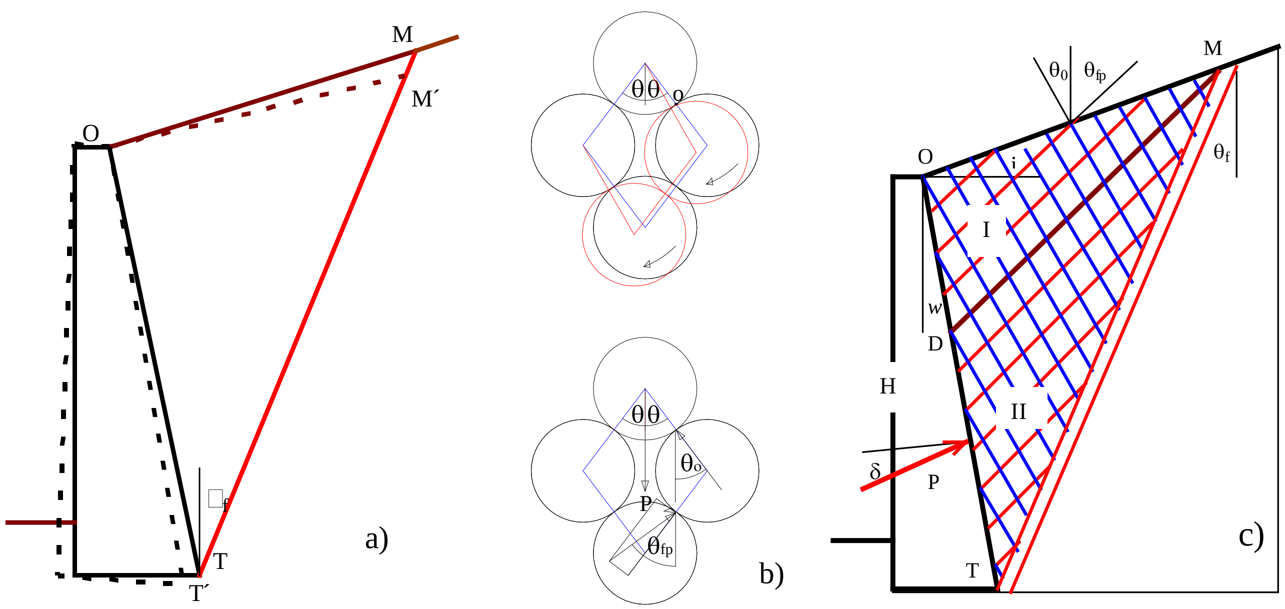

Fig. 3. Example of granular kinematics: retaining wall rotating about the top under moderate earthquake: a) Cinematic boundary conditions; b) Kinematics and statics of the grains in a basic rhomboid cell; and c) Resulting bands of contact forces in the semi-plastic mobilized wedge.

Two mechanisms are plausible. a) Each lower grain rotates clockwise about the point of contact with the upper left grain, remaining, therefore, this contact force at rest, so that, $\theta_1 = \theta_0$ (Fig. 3). But this rotation is only possible if each lower right grain gets to slide upward with respect to the lower left grain. This means that, at failure, the contact force must reach the direction of the passive plastic state; so that $\theta_2 = \theta_{fp}$. b) The upper grain is indented symmetrical and vertically into the pore, and the lower grain rotates clockwise about the point of contact with the upper one. These two movements are only possible if each lower grain slides in the clockwise direction with respect to all the neighboring grains. At failure, $\theta_1 = \theta_f$ and $\theta_2 = \theta_{fp}$. For the two mechanisms, since $\theta_{fp} > \theta_f$, the distribution of the lateral pressure is bilinear with the apex near the top of the retaining wall. In this case, the first mechanism occurs during moderate earthquakes, while the second mechanism is valid for severe earthquakes.

9. Lateral earth pressure on retaining walls

Being known the stresses in the soil mass by the equation 3, the lateral pressure against the retaining wall may be obtained by using the equations of stress transformation, so that in the back face of the retaining wall the boundary condition is met: $\tau = \sigma \tan \delta$, where δ is the soil-wall angle of friction. But this process leads to solve a set of extensive and complicated algebraic equations. To avoid this, an alternative, elegant and simple method is used. First, the unitary lateral force, F_a, is determined as the resultant force of the unitary forces F_1 and F_2 on the back face of the wall. In this context, the force F_2 is known in magnitude and direction, while the unitary force F_1 and the lateral force F_a are known only in direction. Applying the law of sines to this polygon of forces, F_a is obtained in terms of F_2. Second, the area, S, of the subtended section on the wall back face by the band 2, the area S_2 of the base, and the band itself forms a triangle, to which, the application of the law of sines yields the area S in terms of the area F_a. Third, the band 2, the ground surface, and the back side of the wall forms a triangle, whose solution gives z_2 in terms of the depth with respect to the top of the wall, z, in zone I. The band 2, the limit plastic band, and the back side of the wall forms a triangle, which may be solved by using the law of sines to yield z_2 in terms of H-z, in zone II. Finally, substituting these values in equation (2) gives the lateral earth pressure for each zone:

$$\sigma_I = \frac{\gamma(1-\alpha_v) z \sin(\theta_1 + s)\sin(\theta_2 + w)\cos(w - i)}{\cos s \cos w \cos(\theta_2 + i)\cos(\theta_1 - w - \delta)} \tag{7}$$

$$\sigma_{II} = \frac{\gamma(1-\alpha_v)(H - z)\sin(\theta_1 + s)\sin(\theta_2 + w)\cos(\theta_f + w)}{\cos s \cos w \cos(\theta_2 - \theta_f)\cos(\theta_1 - w - \delta)} \tag{8}$$

These equations predict that the lateral pressure increases linearly with depth in the zone I, but decreases in the zone II, grasping the maximum value at the line separating the two zones. The depth of the maximum lateral pressure is denoted by H_I, and it can easily be found in terms of H. Then, replacing z by H_I in Eq. (7), the maximum lateral pressure is found to be:

$$\sigma_{máx} = \frac{\gamma(1-\alpha_v) H \sin(\theta_1 + s)\sin(\theta_f + w)\cos(w - i)}{\cos s \cos w \cos(\theta_f + i)\cos(\theta_1 - w - \delta)} \tag{9}$$

Finally, the lateral force of backfill soil acting against the retaining wall can be attained as the area of the triangle formed by the length of the wall back face, as its base, and the maximum lateral pressure, as its height.

$$P_a = \frac{\gamma H^2}{2} \frac{(1-\alpha_v)\sin(\theta_1 + s)\sin(\theta_f + w)\cos(w - i)}{\cos^2 w \cos \cos(\theta_f + i)\cos(\theta_1 - w - \delta)} \tag{10}$$

10. Point of application

Since the distribution of lateral pressure against the wall has a triangular shape, relations of proportionality between its elements can be established straightforward: for instance, the proportionality between the lateral forces in each zone, and the length of their bases, or the proportionality between the lateral forces in each zone and the total lateral force. In this trend, the depths of the points of application of theses forces are related to each other, in such a way that $H_a = (H+H_I)/3$, where H_a is the point of application of the resultant lateral force. In unfolded fashion:

$$H_a = \frac{H}{3}\left[1 + \frac{\sin(\theta_f + w)\cos(\theta_2 + i)}{\sin(\theta_2 + w)\cos(\theta_f + i)}\right] \quad (11)$$

It is worth to note that this equation does not depend on angle θ_1, while the equation of the earth lateral pressure does not depend on θ_2, and it exhibits a much simpler mathematical structure than Mononobe-Okabe´s.

11. Evaluation of results

11.1 Lo Grasso, Maugeri and Motta

Lo Grasso, Maugeri and Motta [21] reported the experimental results of a series of tests on the shaking table of the University of Catania, with a model of gravity retaining wall, subject to the pressure of a dry granular backfill soil. The models were instrumented to measure displacement, acceleration and dynamic pressure. The retaining walls were built with micro-concrete and were 30 cm high. The soil used in all tests was a dry silica sand of the Sicily east coast, with the following characteristics: $D_{60}/D_{10} = 2.41$, $D_{50} = 0.42$mm, $\gamma_{máx} = 18.27$ kN/m^3, $\gamma_{mín} = 15.04$ kN/m3, $\varphi_p = 37°$, and $D_R = 75\%$. The soil-wall system was subjected to a sinusoidal acceleration whose amplitude was increased with time to reach maximum values of 0.37g and 0.43g, while the frequency was kept constant at 6 Hz (Fig. 4).

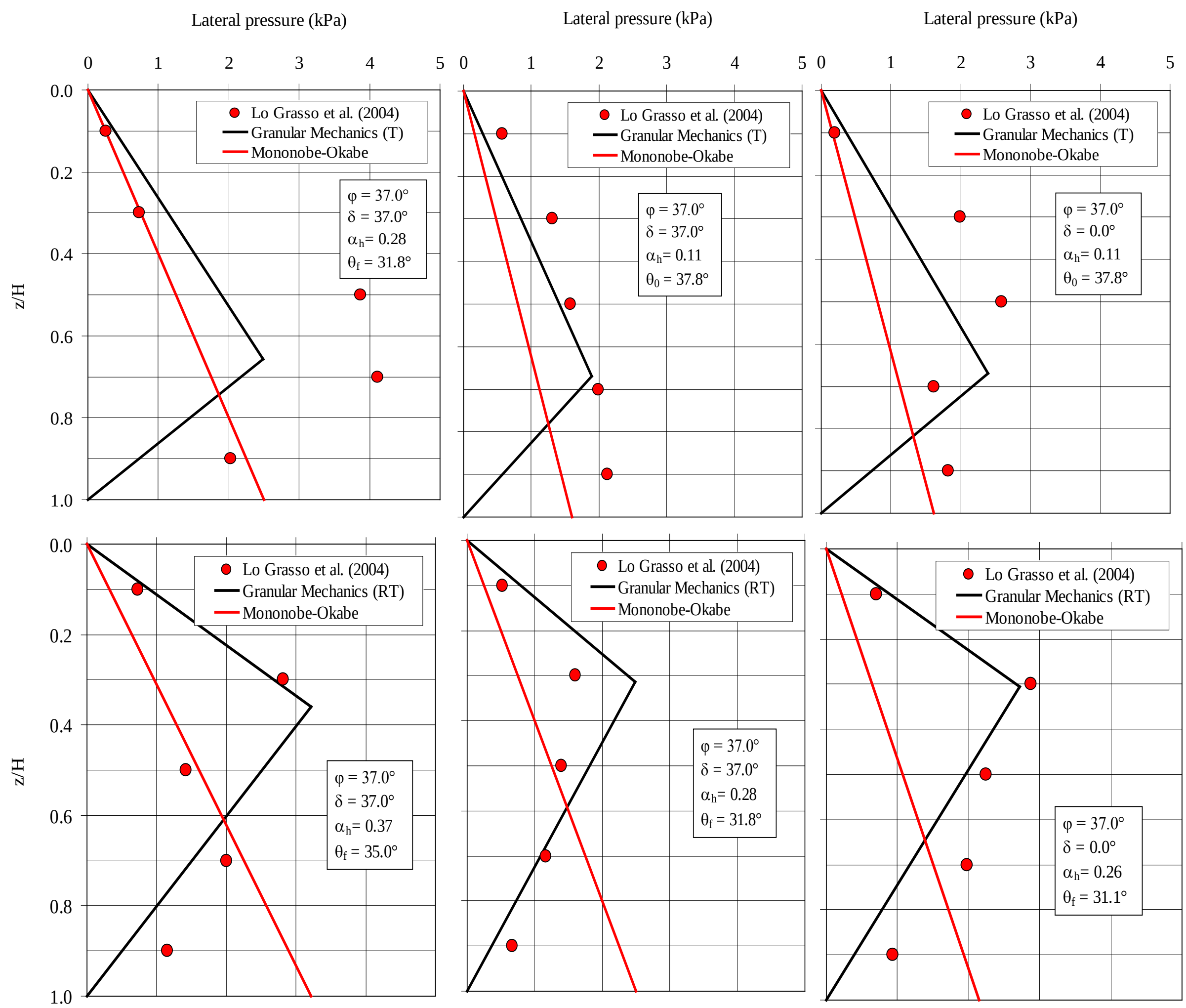

Fig. 4. Distribution of the lateral pressure on a retaining wall that translates horizontally (T), and rotates about the top (RT) [21]

11.2 Sherif and Fang

In figure 5, the points of measurement of the horizontal lateral pressure, reported by Sherif and Fang [22], are shown. The properties of the backfill dense sand were: volumetric weight, 15.99 kN/m^3; peak friction angle, 40.1°; soil-wall friction angle, 20.05°. The retaining wall, that was subject to a sinuoidal acceleration up to 0.52g, was 1.0 m high and rotated around the top (RT).

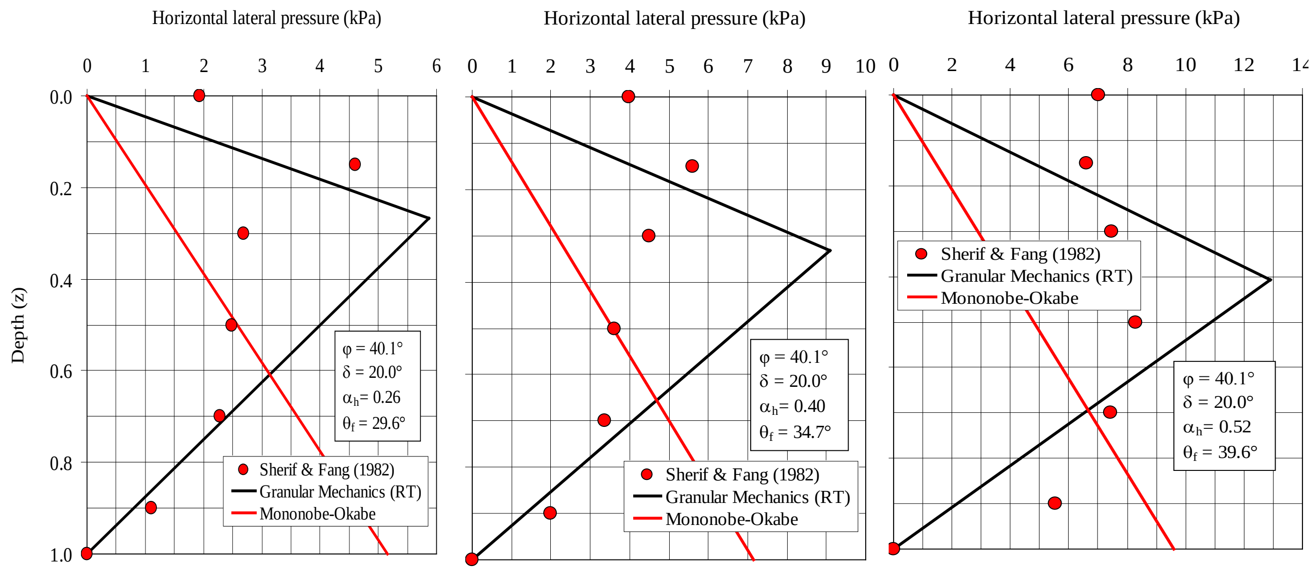

Fig. 5. Distribution of the lateral pressure on a retaining wall that rotates about the top (RT) [22]

11.3. Ishibashi and Fang

Ishibashi and Fang [23] published the results of a set of tests with retaining walls 1.00 meter high subjected to the action of the shaking table at the University of Washington. The backfill soil used was the Ottawa silica sand, with the following properties: unit weight, γ = 15.99 kN/m^3 and φ_p = 40.1°. Two modes of movement of the wall were tested: rotation around the base (RB) and rotation about the stop (RT). As can be seen in figure 6a, the distribution of horizontal lateral pressures under the RB mode matches well with the Mononobe-Okabe method as well as with the granular mechanics that are larger. The experimental value on the wall base is much higher due to the restriction of the grains motion at this point [3]. However, in the RT mode, the best agreement happens with the granular mechanics.

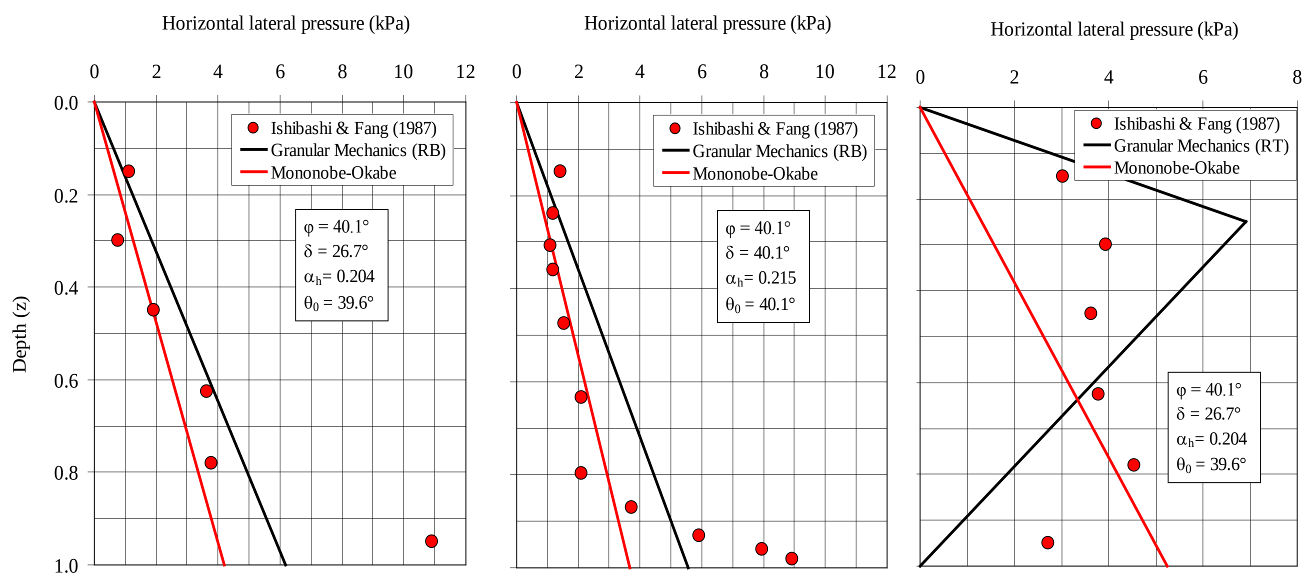

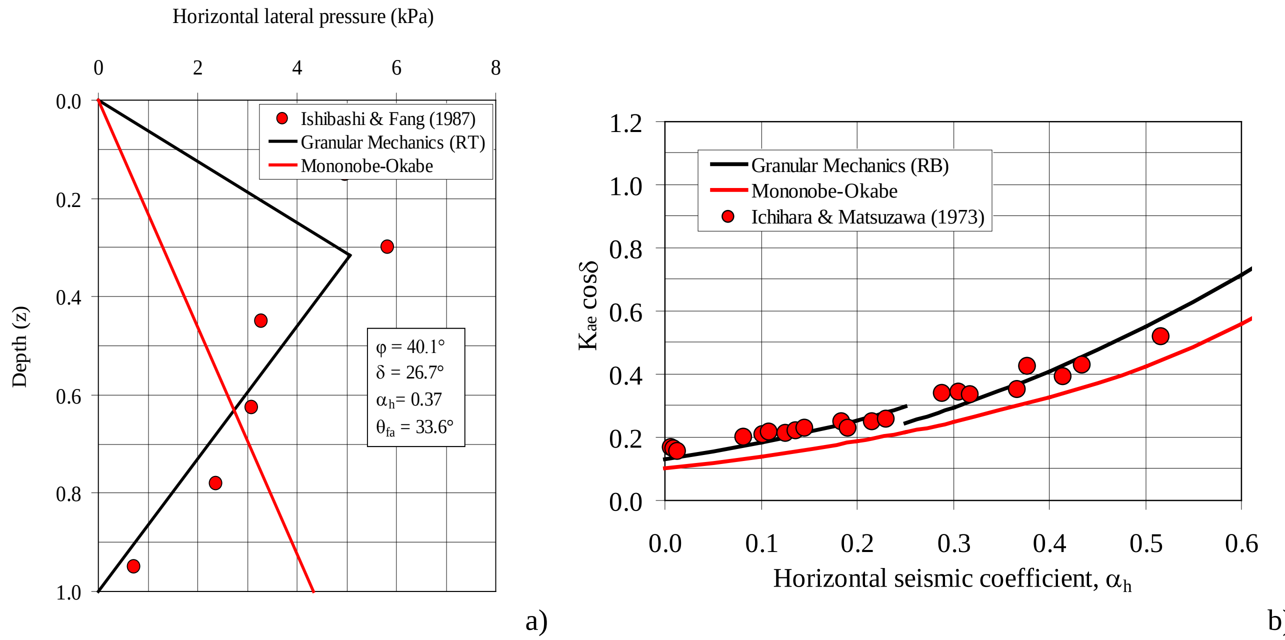

Figure 6.- a) Distribution of the lateral earth pressure on retaining walls rotating about the base and about the top [23]. b) Relationship between the seismic coefficient and the coefficient of the horizontal force [24].

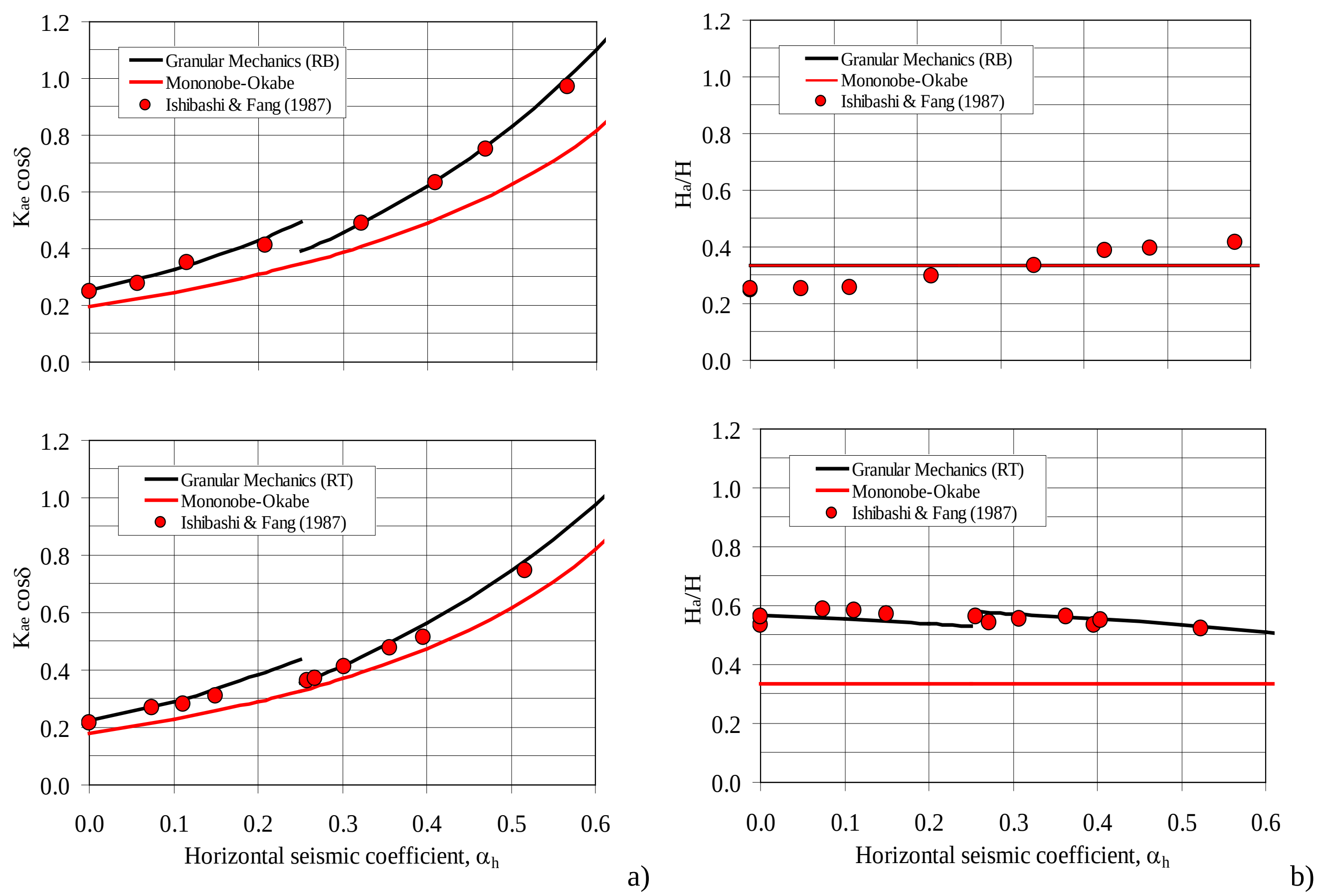

Fig. 7. Relationship between the horizontal seismic coefficient and a) the coefficient of the horizontal lateral force, b) the point of application, for retaining walls rotating about the base (RB), and about the top (RT) [23].

11.4. Ichihara and Matsuzawa

Ichihara and Matsuzawa [24] conducted a shaking table test using a large scale vibrating soil bin to estimate the active lateral pressure during earthquakes. The retaining wall was 0.55 m high, and the soil used was dried Toyoura sand, with an estimated friction angle of φ_p=51°, and a soil-wall friction of 2/3φ, (Fig. 6b).

11.5. Sherif, Ishibashi and Lee

Sherif, Ishibashi and Lee [25] reported the results of a test conducted to measure the active dynamic lateral pressure against a retaining wall 1.0 m high, submitted to a translation mode (T). Backfill soil properties were: unit weight, 16.28 kN/m^3; peak friction angle of 40.9°; soil-wall friction angle, 23.9 °; ground slope, 0°, (Fig.8).

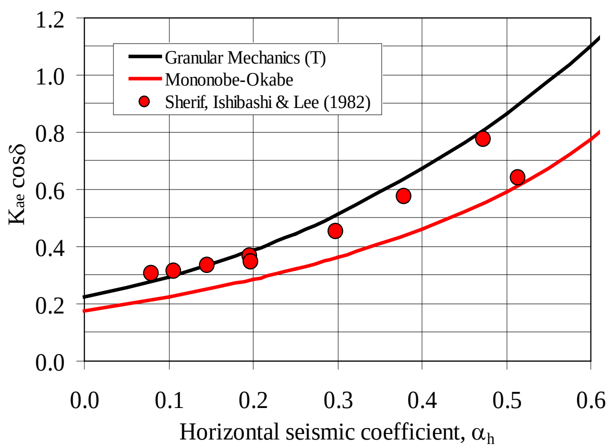

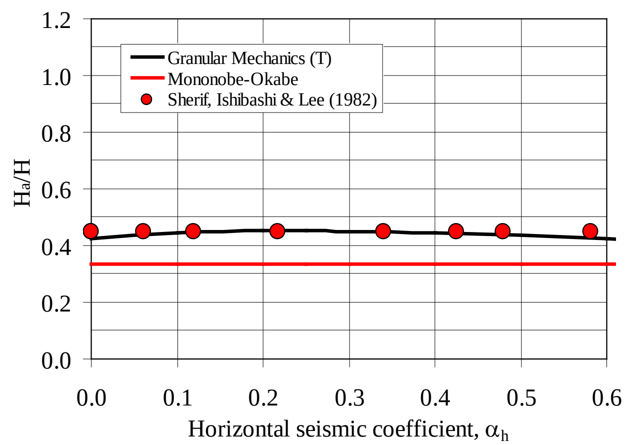

Fig. 8 a) Relationship between the horizontal seismic coefficient and a) the coefficient of the horizontal lateral force, b) the point of application, for a retaining wall that translates horizontally (T) [25]

12. Conclusions

The granular mechanics provides a more accurate and rigorous description of the lateral pressure of a backfill soil on a retaining wall, based on the linear bands of contact forces theory. The formulas, as well as their derivation, are very simple and practical, even for the very general conditions. This theory predicts that the lateral earth pressure distribution is a) linear, when the retaining wall rotates about the base (RB), b) bilinear with the maximum value near the base, when the wall undergoes a translation movement (T); and c) bilinear with the maximum value near the top, if the wall rotates about the top (RT). The calculated distributions coincide with the general tendency of the experimental data reported by several authors, which have a lot of scattering yet. Even though, the coefficients of the earth lateral resultant force obtained from the granular theory match very well with the experimental coefficients; which are known long ago to be always higher than those obtained by the Mononobe-Okabe formula. Likewise, the point of application of the lateral force is found to be 1/3H, in the RB mode; between 0.426H and 0.452H, in T mode; and between 0.538H and 0.579H, in the RT mode; showing very good agreement with the experiments and some Design Manuals specifications, such as 1/3H, 0.45H and 0.55H, respectively. On the other hand, the kinematics of the grains points out that, in both cases of rotation of the wall, two kinds of bands of contact force network are possible, one describing a semi-plastic condition, and the other, a fully plastic state. Correlation of the seismic wave energy and the soil strain energy conduces to relate the first mechanism to moderate earthquakes, and the second, to severe earthquakes; explaining in this way the drift on the experimental and observational data for seismic accelerations larger than 0.25g, approximately.

5. References

[1] Okabe, S. 1924. General theory on earth pressure and seismic stability of retaining walls and dams. *J. Japanese Soc. Civil Eng.* , 10; 1277-1323.

[2] Mononobe, N. and H. Matsuo, 1929. On the determination of earth pressure during the earthquake. *Proceedings of the World Engineering Conference*, pp. 177-185.

[3] Hazarika, H. 2009, Prediction of seismic active earth pressure using curved failure surface with localized strain. *American J. of Eng. And Applied Sciences* 2 (3): 544-558.

[4] Koseki, J., F. Tatsuoka, Y. Munaf, M. Tateyama and K. Kojima, 1998. A modified procedure to evaluate active earth pressure at high seismic loads. Special Issue, *Soil and Found*., 2:209-216.

[5] Zhang, J.M. and D. Li. 2001. Seismic active earth pressure considering the effect of strain localization. *Proc. 4th Int. Conf. on Recent Advances in Geotech. Earthquake Eng. and Soil Dynamics*. Missouri.

[6] Fang Y.S.and T.J. Chen, 1995. Modification of Mononobe-Okabe Theory. *Geotechnique*, 45: 165-167.

[7] Ichihara M. and H. Matsuzawa, 1973. Earth pressure during earthquake. *Soil and Found*., 13: 75-86.

[8] Yanqui, C. 2013. Granular mechanics of the critical state of coarse soils. Proc. *7th. Int. Conf. on Micromechanics of granular media.* AIP 1542, 197-200.

[9] Majmudar, T.S. and R.P. Behringer, 2005. Contact force measurements and stress – induced anisotropy in granular materials. *Nature* 435: 1079.

[10] Snoeijer, J.H., T.J.H. Vlugt, M. van Hecke and W. van Saarloos. 2004. Force network ensemble: a new approach to the static granular matter. *Phys. Rev. Lett*., 92: 054302.

[11] Ostojic, S. 2006. *Statistical mechanics of static granular matter*. Ph. D. Thesis. University of Amsterdam.

[12] Cundall, P.A. and O.D.L. Strack, 1979. A discrete numerical model for granular assemblies. *Geotechnique* 29: 47-65.

[13] Trollope, D.H. 1956. The *Stability of Wedges of Granular Materials*. Ph. D. Thesis. University of Melbourne.

[14] Rowe, P.W. 1962. The stress-dilatancy relation for static equilibrium of an assembly of particles in contact. *Proc. Royal Soc*. , A269: 500-527.

[15] Yanqui, C. 1995. Stresses induced by footings in discontinua. *Proc. 10th. Panamerican Conf. on soil mech. And found*. Vol.3: 1341-1353.

[16] Yanqui, C. 1982. *Statics of gravitating discontinua*. M.Sc. Thesis, University of South Carolina.

[17] Li, J. and M. Ostoja-Starzewski, 2014. Fractal shear bands at elastic-plastic transitions in random Mohr-Coulomb materials. *J. Eng. Mech. ASCE*. 04014072.

[18] Hazarika, H. and H. Matsuzawa. 1997. Coupled shear band method and its application to the seismic earth pressure problems. *Soil and Foundations*, 37: 65-77.

[19] Noda, S.T., T. Uwabe and T. Chiba, 1975. Relation between seismic coefficient and ground acceleration for gravity quay wall. *Repot to Port Harbor Res. Inst*. 14: 67-111.

[20] Matsuo, M. and K. Itabashi, 1984. Study on aseismicity evaluation of slopes and earth structures. *J. JSCE*., 352: 139-147.

[21] Lo Grasso, A. S., M. Maugeri and E. Motta, 2004. Experimental results on earth pressures on rigid wall under seismic condition. *Proc. 13th World Conf. on Earthquake Engineering*. Canada.

[22] Sherif, M. and Y.S. Fang, 1984. Dynamic earth pressure on walls rotating about top. *Soils and Found*, 24(4), 109-117.

[23] Ishibashi, I, and Y.S. Fang, 1987, Dynamic earth pressures with different wall movement modes. *Soil and Found*., 27: 11-22.

[24] Ichihara, M. and H. Matsuzawa, 1973. Earth pressure during earthquake. *Soil and Found*., 13: 75-86.

[25] Sherif, M.A., I. Ishibashi and C.D. Lee, 1982, Earth pressures against rigid retaining walls. *J.Geotech. Eng. ASCE*., 108: 679-696.